Aerosol Science and Technology

ISSN: 0278-6826 (Print) 1521-7388 (Online) Journal homepage: http://www.tandfonline.com/loi/uast20

A Study of the Effects of Anisokinetic Sampling

Daniel J. Rader & Virgil A. Marple

To cite this article: Daniel J. Rader & Virgil A. Marple (1988) A Study of the Effects of Anisokinetic Sampling, Aerosol Science and Technology, 8:3, 283-299, DOI: 10.1080/02786828808959190

To link to this article: http://dx.doi.org/10.1080/02786828808959190

A Study of the Effects of Anisokinetic Sampling

Daniel J. Rader* and Virgil A. Marple
Particle Technology Laboratory, Department of Mechanical Engineering, University of Minnesota, Minneapolis, MN 55455

The results of a numerical investigation of sampling bias through cylindrical probes are presented for both iso- and anisokinetic conditions for thin- and thick-walled probes. Laminar flow fields are calculated using a finite-difference solution of the Navier-Stokes equations; particle trajectories are then calculated with a fourth-order Runge-Kutta method to integrate the particle equation of motion. An ultra-Stokesian drag law and particle interception are included in the calculation. Based on a dimensional analysis of the problem and on the assumptions of the physical model, five dimensionless groups, Re, $\bar{U}/U_o$, D/d, St, and $\rho/(\rho_p C)$ are identified that specify the aspiration coefficient, $A_i = \bar{C}/C_o$. Systematic investigations show that the tube Reynolds number, Re, and the slip-modified density ratio, $\rho/(\rho_p C)$, have only a minor influence in determining A_i. Calculations are made to determine the influence of the remaining groups—velocity ratio ($\bar{U}/U_o$), diameter ratio (D/d), and Stokes number (St)—on the sampling process. For thin-walled probes, the present results are found to be in good agreement with reported experimental data, and with a semiempirical expression proposed by Belyaev and Levin. A least-squares curve-fitting method is used to determine a slightly more accurate correlation. Results for thick-walled probes are found to be in qualitative agreement with reported experimental findings: 1) even isokinetic sampling does not insure a representative sample; 2) probe thickness was found to play a minor role for superisokinetic sampling ($\bar{U}/U_o > 1$); and 3) for subisokinetic sampling ($\bar{U}/U_o < 1$), a thick-walled probe actually provides a sampling efficiency that is closer to unity than a thin-walled probe.

NOMENCLATURE

A_i	aspiration coefficient, $\bar{C}/C_o$
A_i^*	aspiration coefficient for point-mass particles
C	Cunningham slip correction factor
$\bar{C}$	mean concentration at tube inlet, n/cm^3
C_D	drag coefficient
C_o	mainstream concentration, n/cm^3
d	inner diameter of tube, cm
D	outer diameter of tube, cm
D_p	particle diameter, cm
k	coefficient in aspiration equation
r', z'	radial and axial coordinates of particle, cm
r, z	dimensionless coordinates, $r'/d, z'/d$
Re	tube Reynolds number, $\rho d\bar{U}/\mu$
Re_p	local particle Reynolds number
Re_{p,U_o}	particle Reynolds number based on mainstream velocity, $\rho D_p U_o/\mu$
Re_{U_o}	Reynolds number of the undisturbed flow, $\rho dU_o/\mu$
R_p	particle radius
St	Stokes number, $\rho_p D_p^2 U_o C/18\mu d$
t'	time, s
t	dimensionless time, $t'U_o/d$
U_o	mainstream velocity, cm/s
$\bar{U}$	mean tube velocity, cm/s

*D. J. Rader is currently with the Fluid and Thermal Sciences Department, Sandia National Laboratories, Albuquerque, NM 87185.

Aerosol Science and Technology 8:283–299 (1988)

0278-6826/88/$3.50

V_r', V_z'	r and z components of fluid velocity, cm/s
V_r, V_z	dimensionless components of fluid velocity, $V_r'/U_o, V_z'/U_o$
β	coefficient in aspiration equation
μ	fluid viscosity, g/cm/s
ϕ	diameter of limiting trajectory, cm
ρ	fluid density, g/cm^3
ρ_p	particle density, g/cm^3
$\rho/(\rho_p C)$	slip-modified density ratio

INTRODUCTION

The accurate measurement of aerosol size distributions is frequently complicated by the nonideality of the aspiration process. It becomes particularly difficult to extract representative samples when the velocity vectors (both direction and magnitude) characterizing the flows in the sampling probe and ambient fluid differ significantly. Under these conditions, inertial effects can cause particle trajectories to separate from fluid streamlines. The aspirated sample may either over- or underestimate the true concentration, and this discrepancy will vary with both the nature of the flow field and the particle size. Even isokinetic sampling, in which upstream and sample velocity vectors are carefully matched, can result in sampling biases when the probe is "thick walled."

An extensive literature exists on inertial sampling bias; both theoretical (e.g., Badzioch, 1959; Vitols, 1966; Selden, 1975) and experimental work (e.g., Watson and Morris, 1952; Badzioch, 1959; Lundgren and Calvert, 1967; Sehmel, 1967; Zenker, 1971; Belyaev and Levin, 1972; Durham and Lundgren, 1980; Jayasekera and Davies, 1980; Davies and Subari, 1982; Lipatov *et al.*, 1986; Vincent *et al.*, 1986) are well represented. Most of this work has concentrated on "thin-walled" probes, although thick-walled probes are frequently encountered in laboratory air samplers and have also been investigated (Ingham, 1981; Vincent and Mark, 1982; Vincent *et al.*, 1982; Vincent, 1984). Recently, several papers have appeared (Fuchs, 1975; Lutz and Bajura, 1982; Stevens, 1986) that review the literature on the sampling bias resulting from inertial effects.

This work presents the results of numerical calculations of both iso- and anisokinetic sampling through thin- and thick-walled tubes. Laminar flow fields are calculated using finite difference solutions of the Navier-Stokes equations, and particle trajectories are then calculated through an integration of the particle equation of motion. Because of the two-dimensional nature of the solution method, the results are limited to the case of isoaxial sampling (probe facing directly upstream) with a cylindrical tube. The results are compared to previously reported experimental data whenever possible.

PHYSICAL BACKGROUND

A typical sampling geometry is shown in Figure 1. A uniformly distributed aerosol of concentration C_o approaches the sampling tube with the velocity, U_o, of the entraining fluid. A suction characterized by the mean velocity of fluid within the tube, $\bar{U}$, results in the aspiration of both fluid and particles into the sampling tube. The tube has an inner diameter of d, an outer diameter of D, and is shown aligned with its axis parallel to the direction of flow.[1] Inertial effects act upon particles in the vicinity of the tube inlet, and may result in the deviation of particle trajec-

[1] The isoaxial condition is imposed by the present numerical method. The case of anisoaxial sampling has been studied experimentally by Durham and Lundgren (1980), Davies and Subari (1982), Tufto and Willeke (1982), and Vincent *et al.* (1986).

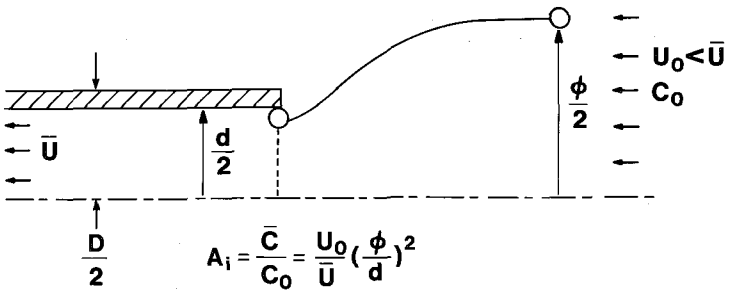

FIGURE 1. Sampling geometry for a cylindrical probe sampling isoaxially.

tories from fluid streamlines. For such cases, the concentration of particles entering the inlet, $\bar{C}$, will differ from the undisturbed upstream concentration.

An inertial aspiration coefficient (A_i) can be defined as the ratio of the particle concentration at the inlet to that upstream:

$$A_i = \frac{\bar{C}}{C_o}. \tag{1}$$

Note that A_i can be either greater or less than unity, depending on the nature of the flow field. For example, Figure 1 shows a possible particle trajectory under superisokinetic sampling conditions ($\bar{U} > U_o$). A critical trajectory (for a particle that just enters the tube) is shown. A slightly larger particle starting from the same initial location would not be sampled, but would be intercepted by the lip of the probe. In the limit of infinite mass, a particle would stream past the sampler unperturbed. Thus, for superisokinetic sampling of large particles, the concentration at the entrance to the sampling tube would be depleted relative to that upstream ($A_i < 1$). Inertial effects during subisokinetic sampling ($\bar{U} < U_o$) can lead to an enrichment of the large-particle concentrations at the tube inlet ($A_i > 1$).

Sampling bias can also result from factors other than inertial separation: 1) Solid particles may rebound from the leading edge or outer walls of the tube and be subsequently drawn in with the sample, thus increasing the inlet concentration. Lipatov *et al.* (1986) used the limiting trajectory method to experimentally determine the magnitude of secondary aspiration due to particle bounce for a limited number of cases. They found that particle bounce became increasingly important for larger particles, smaller diameter probes, and higher velocity ratios ($\bar{U}/U_o$). 2) Depending on tube orientation, particle settling due to gravity can either increase or decrease the concentration entering the probe (Tufto and Willeke, 1982). 3) Once past the entrance plane of the tube, particle deposition on interior surfaces continuously reduces the concentration. Stevens (1986) divided deposition losses into two regions: that occurring near the nozzle entrance and that occurring along the remaining length of tube. The former depends on the flow field upstream of the inlet and thus is closely related to the aspiration process, while the latter depends on the nature of the flow within the tube and is essentially independent of inlet conditions. Sampling bias resulting from deposition has been investigated by several workers (e.g., Belyaev and Levin, 1974; Durham and Lundgren, 1980; Jayasekera and Davies, 1980; Davies and Subari, 1982; Tufto and Willeke, 1982). To minimize deposition bias, Belyaev and Levin (1974) argue that the inlet hole diameter must be sufficiently large to ensure that the deposited particles constitute only a small fraction of the total sample ($d > 1.0$ cm).

Particle deposition, rebound, and sedimentation have not been considered in the present work. These restrictions, however, do

not all represent limitations of the numerical method. Inertial deposition within the tube could be easily handled, as could the influence of gravity if it acted parallel to the tube axis. Particle rebound could be included with the use of a particle–surface interaction model. Anisoaxial gravity cannot be handled with the current model since it makes the problem three dimensional. Thus, in this work, the concentration $\bar{C}$ includes only those particles that arrive at the entrance plane of the tube as the result of aerodynamic and inertial forces.

The shape of the probe plays a major role in its overall sampling performance. For cylindrical tubes, the main parameter of interest is the wall thickness. Belyaev and Levin (1974) separated sample inlets into two classes: thin- or thick-walled. For an ideal thin-walled probe sampling isoaxially and isokinetically, there would be no disturbance of the ambient flow and the aspiration coefficient would be one. In practice, a probe is considered thin-walled if its aspiration coe fficient is sufficiently close to one under isoaxial, isokinetic conditions. Belyaev and Levin (1974) experimentally determined that a probe can be regarded as thin-walled when the ratio of its outer to inner diameter is < 1.1 ($D/d < 1.1$). In this work, the sampling behavior of both thin- and thick-walled cylindrical probes is investigated.

PREVIOUS WORK

The earliest experimental work (Brady and Touzalin, 1911) established the qualitative result that sampling with a mean suction velocity different from the upstream velocity leads to sampling error. Badzioch (1959) showed experimentally that the aspiration coefficient, $A_i = \bar{C}/C_o$, depended on the velocity ratio, $\bar{U}/U_o$, and a dimensionless inertial parameter, taken as the Stokes number St, which is

$$\mathrm{St} = \frac{\rho_p D_p^2 U_o C}{18 \mu d}, \tag{2}$$

where ρ_p = particle density, D_p = particle diameter, C = Cunningham slip correction factor, d = inner diameter of sampling tube, and μ = fluid viscosity. Although the use of St as the appropriate inertial parameter is widely accepted, some workers (e.g. Selden, 1975, 1977) have suggested correlating sampling data with both St and the particle Reynolds number, Re_{p,U_o}, where

$$\mathrm{Re}_{p,U_o} = \frac{\rho D_p U_o}{\mu}, \tag{3}$$

and ρ is the fluid density. It will be shown later that both Re_{p,U_o} and St are required to completely describe particle trajectories. However, for the class of problems considered here, we will show that the Stokes number is the dominant parameter, and that A_i is only weakly dependent on Re_{p,U_o}.

Vitols (1966) used numerical methods to obtain theoretical estimates of sampling errors that were in good agreement with Badzioch's data. He first applied a finite-difference method to solve a Laplace-type stream-function equation for the flow field (frictionless, ideal fluid), and then integrated the particle equation of motion to obtain particle trajectories. From these calculations, he reported the aspiration coefficient as a function of $\bar{U}/U_o$ and St. Unfortunately, only results for $\mathrm{St} > 2$ are given. This St range is of limited interest, since particle trajectories are nearly straight and A_i is only a weak function of St.

The exact functional relationship for the aspiration coefficient was not easily expressed due to the scatter inherent in these early experiments. Attempts to calculate the sampling efficiency from measured flow fields (Ruping, 1968) did not yield the desired functional form either. Later work (Sehmel, 1967; Lundgren and Calvert, 1967; Zenker, 1971; Belyaev and Levin, 1972; Durham and Lundgren, 1980; Jayasekera and Davies, 1980; Davies and Subari, 1982; Vincent *et al.*, 1986) provided more reliable data. Belyaev and Levin (1972) explained the remaining discrepancies among the various ex-

perimental investigations as resulting from uncertainties in 1) particle deposition within the probe, 2) particle rebound from the leading edge of the probe, and 3) thick-walled sampling probes. Using a flash illumination photographic method which minimized these uncertainties, Belyaev and Levin (1972) investigated the dependence of the inertial aspiration coefficient on $\bar{U}/U_o$, St, and D/d.

In a subsequent paper (Belyaev and Levin, 1974), these same authors discuss approximate formulas for the aspiration coefficient. The following form was first reported by Watson and Morris (1952) who attributed it to C.N. Davies (see also Badzioch, 1959; Davies, 1968; Zenker, 1971):

$$A_i = 1 + \beta\left[\frac{U_o}{\bar{U}} - 1\right], \tag{4}$$

where β is a coefficient that depends on the dimensionless Stokes number, and may also depend on other factors. Two asymptotic limits for β are easily understood. First, in the limit of zero mass ($St \to 0$), particles may be expected to exactly track fluid streamlines, resulting in an aspiration coefficient of one and requiring that $\beta \to 0$ as $St \to 0$. Second, because of their inertia, large particles ($St \to \infty$) persist on straight trajectories (in their original directions) independent of the changes in the flow field near the probe inlet. In this case, it is easily shown that the aspiration coefficient approaches $U_o/\bar{U}$, so that $\beta \to 1$ as $St \to \infty$.

Analysis of Ruping's (1968) results, however, suggests that the function β also depends on the velocity ratio $\bar{U}/U_o$. Although Ruping's results did not permit a determination of this relationship, those of Belyaev and Levin (1972) did. This was accomplished by modifying a formula originally proposed by Davies (1968):

$$A_i = 1 + \left[\frac{U_o}{\bar{U}} - 1\right]\left[1 - \frac{1}{1 + k\mathrm{St}}\right], \tag{5}$$

where k was a constant determined from experimental data. Belyaev and Levin (1974) suggested that k was not constant, but varied with the velocity ratio. Their data ($0.18 < St < 2.03$) supported the following linear relationship between k and the velocity ratio:

$$k = 2 + 0.62\frac{\bar{U}}{U_o} \qquad 0.2 < \bar{U}/U_o < 6. \tag{6}$$

Stevens (1986) found Eqs. (5) and (6) gave values of A_i within 10% of the recent experimental data of Davies (Jayasekera and Davies, 1980; Davies and Subari, 1982) for $0.05 < St < 1.0$, and supported the extension of the correlation into this St range. Durham and Lundgren (1980) and Lipatov *et al.* (1986) also found excellent agreement between their data and the Belyaev and Levin correlation. Martone *et al.* (1980) reported data that were in good agreement with Eqs. (5) and (6) even for subisokinetic sampling from near-sonic and supersonic free jets.

For $\bar{U}/U_o > 5$, large discrepancies are found between Davies' results (Jayasekera and Davies, 1980; Davies and Subari, 1982) and the correlation of Eqs. (5) and (6). To account for such differences, Davies and Subari proposed a new correlation for β whereas Stevens (1986) recommended Eq. (5) with $k = 2$. Recently, Lipatov *et al.* (1986) reported experimental data that agreed with the Belyaev and Levin correlation for velocity ratios $\bar{U}/U_o$ as large as 35. Unlike Davies' data, which included particles sampled through primary aspiration as well as secondary aspiration due to particle bounce, Lipatov's limiting trajectory method (based on photographing of individual particle tracks) minimized the effect of particle bounce. They conclude that the differences observed between Davies' data and the Belyaev and Levin correlation result from particle-bounce interference in the former. Thus, Eqs. (5) and (6) should provide a good correlation for the pure-inertial aspiration coefficient, whereas correlations such as suggested by Davies and Subari (1982) would include both inertial and particle-bounce effects. Since particle–surface interactions can vary significantly between experimental setups, caution should be applied in pre-

dicting aspiration coefficients when significant particle bounce is expected (e.g., solid particles, $\bar{U}/U_o > 5$, or large values of St).

After a statistical examination of their data, Vincent *et al.* (1986) found little evidence to support a velocity ratio dependence in k. They assumed that k is a constant, and gave a best-fit value of $k = 2.1$ for their data. Using a similar analysis on other data sets, they gave values of $k = 1.34$ for that of Durham and Lundgren (1980) and $k = 1.81$ for that of Davies and Subari (1982). After combining all three data sets, their analysis yielded an overall best-fit estimate of $k = 1.8$. Vincent and co-workers noted that the theoretical predictions for A_i using Eq. (5) were relatively insensitive to variations in k under their experimental conditions (variations in k of as much as 30% resulted in differences of the prediction for A_i of $< 10\%$). Part of this insensitivity results from the low range of Stokes number (St < 0.7) investigated.

Several studies have been performed to determine if the aspiration efficiency depends on fluid parameters besides the velocity ratio $\bar{U}/U_o$. Lipatov *et al.* (1986) claimed that measured values for A_i were essentially independent of the Reynolds number of the undisturbed flow ($\mathrm{Re}_{U_o} = \rho U_o d/\mu$) over a wide range ($200 < \mathrm{Re}_{U_o} < 10^5$). Based on theory and experimental data, Vincent *et al.* (1985) concluded that freestream turbulence should not substantially affect the performance of thin-walled probes during isokinetic sampling. They also found the performance of thick-walled probes to be turbulence-independent for small particles (typically < 40 μm), although turbulence effects might be expected for larger particles. Such results suggest that the velocity ratio is the dominant fluid parameter affecting sampling efficiencies.

SOLUTION TECHNIQUES

The general procedure for theoretically determining the effects of anisokinetic sampling is to first analyze the flow field in the absence of particles, and then to determine the trajectories of particles within the flow field. This method requires the assumptions of a dilute aerosol and small particles. In this study a finite-difference method is used to solve the Navier-Stokes equations for the flow field in the vicinity of the probe. This method includes viscous effects, but assumes an axisymmetric, isothermal, incompressible, steady, laminar flow of constant density and viscosity. A cylindrical geometry is also imposed (see Figure 1). Once a flow field is calculated, particle trajectories are determined by numerically integrating the particle's equations of motion. Body forces (e.g., electrical and gravitational) are neglected. Details of the method (including the listing of a FORTRAN implementation) are given in Marple (1970) for the similar case of particle flow through an inertial impactor.

Flow Field

A finite-difference solution developed by Gosman *et al.* (1969) and applied to inertial impactors by Marple (Marple, 1970; Marple *et al.*, 1974) is used to solve the stream–function/vorticity form of the Navier-Stokes equations. The equations are solved in dimensionless form by using the sampling probe inner diameter, d, and the mean tube velocity, $\bar{U}$, as the characteristic length and velocity, respectively. One advantage of this method is that it can be directly applied to the ideal case of a probe of zero thickness.

Care was taken to ensure that the calculation domain was sufficiently large so that the assumption of a uniform flow could be made at the upstream and far-radial boundaries. The domain typically extended five diameters upstream of the probe inlet, a distance suggested by previous workers (e.g., Ruping, 1968; Belyaev and Levin, 1974) for which undisturbed flow prevails. Inspection of calculated flow fields supported this assumption. In the radial direction, the grid was extended sufficiently far as to guarantee that the volume of flow drawn into the probe represents $< 5\%$ of the flow entering the domain. Tests showed this criterion to be

sufficient to allow a uniform-velocity assumption at the far-radial boundary.

The result of the finite-difference solution is an array of velocity components at the node points of a grid covering the area of interest. These velocity components are stored in a data array, and are provided as input to the trajectory solver described next.

Particle Trajectory Calculations

Once a flow field has been calculated, the determination of the aspiration coefficient requires that the trajectories of particles entrained in the flow be calculated. Marple and Liu (1974) presented a method of calculating particle trajectories which used a Runge-Kutta fourth-order method to integrate the equations of particle motion from a given initial position. Marple and Liu assumed that the particles were point masses that experienced drag according to Stokes law, which strictly applies only for particles which move through a still fluid at a constant velocity and at a low local-particle Reynolds number ($\mathrm{Re}_p \ll 1$).[2]

Radar and Marple (1985) improved the method by considering ultra-Stokesian and particle interception effects. First, ultra-Stokesian fluid resistance is accounted for by including an empirical drag coefficient, C_D, in the particle equations of motion. Friedlander (1977, p. 106) gives the following set of dimensionless, differential equations for particle motion in two dimensions:

$$\mathrm{St}\frac{d^2r}{dt^2} = \frac{C_D\mathrm{Re}_p}{24}\left[V_r - \frac{dr}{dt}\right];$$

$$\mathrm{St}\frac{d^2z}{dt^2} = \frac{C_D\mathrm{Re}_p}{24}\left[V_z - \frac{dz}{dt}\right], \qquad (7)$$

where

$$\mathrm{Re}_p = \mathrm{Re}_{p,U_o}\left[\left(V_r - \frac{dr}{dt}\right)^2 + \left(V_z - \frac{dz}{dt}\right)^2\right]^{1/2}; \qquad (8)$$

$$\mathrm{Re}_{p,U_o} = \frac{\rho D_p U_o}{\mu};$$

$$C_D = C_D(\mathrm{Re}_p). \qquad (9)$$

In Eq. (7), second-order terms that account for fluid accelerations have been neglected as suggested by Fuchs (1964, p. 75). In this case, the drag acting on the particle at any location can be calculated using a steady-state drag law with the local instantaneous relative velocity. Steady-state drag coefficients can be obtained from C_D versus Re_p data reported in the literature. Note that Stokes law corresponds to the special case for which $C_D = 24/\mathrm{Re}_p$. For the present work, a correlation of C_D versus Re_p for spherical particles, proposed by Sartor and Abbott (1975), is used for $\mathrm{Re}_p \le 5$; and one proposed by Serafini (Friedlander, 1977, p. 105) for $\mathrm{Re}_p \ge 5$.

$$C_D = \begin{cases} \dfrac{24}{\mathrm{Re}_p}(1 + 0.0916Re_p) & \mathrm{Re}_p \le 5 \\ \dfrac{24}{\mathrm{Re}_p}\left(1 + 0.158\mathrm{Re}_p^{2/3}\right) & \\ & 5 \le \mathrm{Re}_p \le 1000 \end{cases} \qquad (10)$$

The second improvement offered by Rader and Marple (1985) was to omit the assumption of a point-mass particle and include interception effects. Although a minor factor for small particles, interception can become important for larger ones. In the present work, a particle is removed from the flow if its center comes within one particle radius of any solid boundary.

With the above method for calculating particle trajectories, the determination of an aspiration coefficient reduces to finding the diameter, ϕ, of the limiting particle trajectory. The limiting trajectory divides those particles that will enter the sampling tube from those that will not, as depicted in Figure 1. For ϕ measured sufficiently far up-

[2] Both the local-particle Reynolds number based on the instantaneous, relative velocity between the fluid and particle, Re_p, and the particle Reynolds number based on the average velocity of the undisturbed, Re_{p,U_o}, are used in this paper as defined in Eqs. (8) and (9). The former varies with particle location, while the latter is a constant.

stream of any disturbance, the following relation may be used to calculate the aspiration coefficient:

$$A_i = (U_o/\bar{U})(\phi/d)^2. \quad (11)$$

In the numerical model, ϕ was obtained as follows. A particle with a fixed Stokes number is introduced into the flow far upstream of the sample probe at some initial distance from the centerline. The trajectory of the particle is then calculated to determine if it entered the sampling probe. If it did, the particle is again started far upstream at a slightly greater distance from the centerline. If the particle was not sampled by the probe, the particle was restarted from nearer the centerline. This procedure iterates until the diameter of the limiting trajectory is determined to an acceptable precision.

DIMENSIONLESS PARAMETERS

According to classical dimensional analysis (e.g., Van Driest, 1946), the 11 variables that specify the anisokinetic sampling problem (C_o, U_o, $\bar{C}$, $\bar{U}$, d, D, ρ, μ, D_p, ρ_p, and C) can be combined into eight independent, dimensionless groups that completely describe the problem. The Buckingham π theorem (Buckingham, 1914) states that the problem solution can be written in the following functional form:

$$A_i = \frac{\bar{C}}{C_o} = F\left(\mathrm{Re}, \frac{\bar{U}}{U_o}, \frac{D}{d}, \frac{\frac{\pi}{6}D_p^3\rho_p C_o}{\rho}, \mathrm{St}, \frac{\rho}{\rho_p}\frac{1}{C}, C\right) \quad (12)$$

where all terms have been previously defined except the fluid Reynolds number based on the mean sample velocity ($\mathrm{Re} = \rho\bar{U}d/\mu$). Any set of eight groups is allowed provided they are mutually independent; the set specified in Eq. (12) is considered the most appropriate for the present problem.

The fourth group specified in Eq. (12) equals the mass ratio of particulate to air. Under the dilute-solution approximation imposed earlier, this group will have little influence on the aspiration coefficient and may be neglected. This assumption also permits the decoupling of the sampling problem into two steps: 1) the calculation of a Navier-Stokes flow field that is unaffected by the presence of the suspended phase, and 2) the integration of the particle equation of motion. The first three dimensionless groups given in Eq. (12) can be associated with the flow calculation. The Reynolds number is well known to specify laminar flow through a tube, and the velocity and diameter ratios are required to account for complications due to the upstream flow field and tube thickness, respectively.

The final three groups given in Eq. (12) characterize the particle–fluid interaction, which, in the present case, is described by Eqs. (7)–(10). Under this physical description, the slip coefficient C appears only within St, and can thus be neglected as an independent group. Under the above assumptions, Eq. 12 implies that, for a specific flow field, only two dimensionless groups are required to specify the particle trajectory. This is consistent with Eqs. (7)–(10), in which two dimensionless groups (St and Re_{p,U_o}) explicitly appear, although the inclusion of particle interception introduces another dimensionless group (the interception parameter, R_p/d) implicitly. It is easily shown, however, that the interception parameter and particle Reynolds number are not independent, being related for a specific flow field as follows:

$$\mathrm{Re}_{p,U_o} = 2\,\mathrm{Re}\frac{U_o}{\bar{U}}\frac{R_p}{d}. \quad (13)$$

In this work, we have followed the practice of Rader and Marple (1985) and used St and $\rho/(\rho_p C)$ as the appropriated groups. The selection of St is a standard one, and the use of the slip-modified density ratio instead of either the particle Reynolds number or interception parameter is made on practical

grounds. For most aerosol systems, the slip correction is close to and generally assumed to be unity, in which case this chosen parameter simply reduces to a density ratio. Inasmuch as the particle and air densities are frequently constants, it is felt that presenting the aspiration coefficient versus St at fixed values of the density ratio would be of practical use in typical applications. For calculation purposes, particle Reynolds number may be obtained using Eq. (13), while the interception parameter may be obtained through the following relation:

$$\frac{R_p}{d} = \sqrt{\frac{9}{2}\frac{\rho}{C\rho_p}\frac{\overline{U}}{U_o}\frac{\mathrm{St}}{\mathrm{Re}}}\,. \tag{14}$$

RESULTS

In the course of this study, a systematic investigation of the effects which contribute to sampling bias was performed. For a given set of conditions, including probe geometry, velocity ratio, Reynolds number, and particle properties, a determination of the value of the aspiration coefficient is made for 10 values of St in the range from 0.005 to 10. The effects of individual parameters are discussed in the following sections, which fall into two categories: 1) The first two sections deal with variations in the numerical method, including grid refinement and the use of an ultra-Stokesian drag law. 2) The final sections investigate the effect of sampling parameters (e.g., $\overline{U}/U_o$, Re, and D/d) on the aspiration coefficient.

Grid Refinement

For numerical solutions, the accuracy of the final result is related to the number of node points contained within the grid. Thus, an estimate of the discretization error may be obtained by performing calculations with grids of increasing fineness (greater number of grid points). A base grid of 34×48 grid lines was first applied and the aspiration coefficient calculated for each of 10 values of St. This grid was refined by doubling the number of grid lines in each direction and the run was repeated. This process was repeated again, resulting in a grid four times finer than the base case. These three levels of grid refinement are subsequently referred to as standard, double, and quadruple grids.

Grid refinement studies were made at velocity ratios of $\overline{U}/U_o = 5$, 2.5, and 0.1, and the results are given in Table 1. A thin-walled nozzle with a Reynolds number of 300 was used in each calculation, and a slip-modified density ratio of $1.2 \cdot 10^{-3}$ (e.g., $\rho = 1.2 \cdot 10^{-3}$ g/cm^3, $\rho_p = 1$ g/cm^3, and $C = 1$) was as-

TABLE 1. Effect of Grid Refinement

Re = 300 $\rho/(\rho_p C) = 1.2 \cdot 10^{-3}$ Ultra-Stokesian drag

	Aspiration coefficient, A_i								
	$\frac{\overline{U}}{U_o} = 5$			$\frac{\overline{U}}{U_o} = 2.5$			$\frac{\overline{U}}{U_o} = 0.1$		
St	SNGL	DBLE	QUAD	SNGL	DBLE	QUAD	SNGL	DBLE	QUAD
0.005	0.959	0.976	0.976	—	0.974	0.974	1.23	1.26	1.20
0.02	0.925	0.925	0.942	—	0.926	0.938	1.32	1.36	1.27
0.05	0.859	0.843	0.843	—	0.856	0.856	1.53	1.60	1.50
0.10	0.720	0.720	0.720	—	0.778	0.778	1.99	2.15	2.16
0.20	0.606	0.593	0.593	—	0.694	0.694	3.65	3.71	3.69
0.50	0.454	0.443	0.443	—	0.590	0.590	5.76	5.88	5.87
1.0	0.365	0.355	0.355	—	0.517	0.517	7.14	7.26	7.26
2.0	0.300	0.281	0.281	—	0.465	0.465	8.19	8.29	8.28
5.0	0.228	0.228	0.228	—	0.416	0.416	9.05	9.09	9.09
10.0	0.199	0.199	0.199	—	0.378	0.378	9.36	9.40	9.40

sumed. The greatest error would be expected in the extreme values (5 and 0.1), since gradients in the flow field would be largest. For velocity ratios greater than one, however, the effect of grid refinement is small, typically $< 1\%$. In this case, even the single grid gives an acceptable result.

For velocity ratios less than one, discretization errors of as much as 6% in A_i were observed between calculations with double and quadruple grids. It is felt that this error could be explained by considering the nature of the flow field for low velocity ratios. In this case, the fluid being sampled is drawn from an area near the centerline which is smaller than the inlet opening. The details of this small domain are essential to the final result, and require the higher precision of a refined grid.

In the following work, double grids were generally used. Although greater accuracy can be gained from grid refinement, the increased computational costs outweigh the marginal improvements indicated by these refinement studies.

Ultra-Stokesian Drag Law

Several calculations were performed to compare the results from a more accurate drag coefficient [Eq. (10)] with that assuming Stokes law ($C_D = 24/\mathrm{Re}_p$). Except for the drag coefficient used, each set of runs was performed under identical conditions (Re = 2000, $\rho/(\rho_p C) = 1.2 \cdot 10^{-3}$, thin-walled probe). The largest deviations from Stokes law are expected for large values of the particle Reynolds number [see Eqs. (8)–(10)]. From Eqs. (13) and (14), Re_{p,U_o} is seen to increase with increasing St, $\rho/(\rho_p C)$, and Re, and to decrease with increasing velocity ratios. Note that the Re and velocity ratio dependence can be simplified since they only appear as the product $\mathrm{Re} \cdot U_o/\bar{U}$, which defines a Reynolds number based on the undisturbed velocity, Re_{U_o}. Ultra-Stokesian effects are reduced when the undisturbed Reynolds number is kept small.

TABLE 2. Effect of Ultra-Stokesian Drag Law

	Re = 2000 $\rho/(\rho_p C) = 1.2 \cdot 10^{-3}$			
	Aspiration coefficient, A_i			
	$\frac{\bar{U}}{U_o} = 5$		$\frac{\bar{U}}{U_o} = 0.1$	
St	STOKES	Eq. (10)	STOKES	Eq. (10)
0.005	0.959	0.959	1.255	1.255
0.02	0.925	0.925	1.370	1.370
0.05	0.827	0.827	1.614	1.614
0.10	0.705	0.720	2.192	2.118
0.20	0.593	0.593	3.825	3.481
0.50	0.443	0.454	6.063	5.545
1.0	0.355	0.365	7.493	6.929
2.0	0.281	0.300	8.526	8.023
5.0	0.228	0.245	9.318	8.970
10.0	0.212	0.228	9.595	9.364

Comparisons were made at high and low velocity ratios ($\bar{U}/U_o = 5$ and 0.1) at Re = 2000 (the highest Re allowed by the model requirement of laminar flow); the results are given in Table 2. At the higher velocity ratio, the Stokesian assumption is quite accurate except at very large St values. For the low velocity ratio, however, we see deviations of 10% for St values as low as 0.2.

Note that the aspiration coefficient predicted using the ultra-Stokesian drag law always either equals the Stokes law result or is closer to unity than it. This is easily understood by looking at the ultra-Stokesian correlation of Eq. (10), which shows that the Stokes assumption always underpredicts C_D and hence the drag acting on the particle. During trajectory calculations, local particle Reynolds numbers as high as 20 were recorded which would result in an underestimate of the drag force by more than a factor of 2. Since a larger drag force causes particles to more closely follow fluid motions, the ultra-Stokesian particles will show a tendency toward less sampling bias (A_i closer to unity).

The results of these calculations suggest that ultra-Stokesian drag effects need to be included, particularly for low velocity ratios. Thus, the drag correlation of Eq. (10) was used in all of the following calculations.

Reynolds Number Dependence

The tube Reynolds number, Re, enters the sampling-bias calculation in several ways. First, for a given velocity ratio and probe diameter ratio, the value of Re uniquely specifies a flow field (see the preceding section, *Dimensionless Parameters*). Once a flow field has been determined, Re also plays a role in the particle trajectory calculation: Re appears in the expression for both the interception parameter [Eq. (14)] and the particle Reynolds number [Eq. (13)]. Although each of these effects could be investigated separately, we were most interested in determining their combined effect on the aspiration coefficient.

In order to determine these effects, a set of calculations was made at Re values of 300 and 2000 for two velocity ratios (5 and 0.1). These results are given in Table 3. For high velocity ratios, the effect of Re on A_i is very small except for larger St values. This is predominately an interception effect, since the interception parameter increases with velocity ratio and Stokes number [Eq. (14)]. If A_i is adjusted using the interception correction introduced in a later section, the difference between the Re = 300 and 2000 cases essentially vanishes (< 3%).

For low velocity ratios, the effect of Reynolds number is most noticeable at intermediate St values. As the velocity ratio decreases, the interception effect is diminished, but the particle Reynolds number increases [Eq. (13)]. All other conditions held the same, the particle with the larger particle Reynolds number will experience a larger drag, and will more accurately track fluid streamlines (A_i closer to unity). This trend is seen in the data, although the maximum error is still < 6%. For the range of parameters investigated here, these data suggest that Re only weakly influences the aspiration coefficient; this agrees with the experimental conclusions of Lipatov *et al.* (1986).

TABLE 3. Effect of Probe Reynolds Number

$\rho/(\rho_p C) = 1.2 \cdot 10^{-3}$		Ultra-Stokesian drag			
		Aspiration coefficient, A_i			
		$\frac{\bar{U}}{U_o} = 5$		$\frac{\bar{U}}{U_o} = 0.1$	
St	Re =	300	2000	300	2000
0.005		0.976	0.959	1.255	1.255
0.02		0.925	0.925	1.358	1.370
0.05		0.843	0.827	1.601	1.614
0.10		0.720	0.720	2.147	2.118
0.20		0.593	0.593	3.708	3.481
0.50		0.443	0.454	5.879	5.545
1.0		0.355	0.365	7.262	6.929
2.0		0.281	0.300	8.294	8.023
5.0		0.228	0.245	9.091	8.970
10.0		0.199	0.228	9.395	9.364

Slip-modified Density Ratio

In many aerosol sampling systems, the slip-modified density ratio $\rho/(\rho_p C)$ does not vary greatly. Sampling is frequently performed in air near atmospheric conditions and for particles sufficiently large so that C is approximately unity. Under these assumptions, the particle density plays the primary role in determining the density ratio. In the present study, we consider a particle density range of 0.5–10.0 g/cm^3, which covers a large fraction of the frequently encountered aerosol materials. Since both the interception parameter and the particle Reynolds number depend on the square root of $\rho/(\rho_p C)$ [see Eqs. (13) and (14)], it was expected that this parameter would have only a weak influence on A_i. This hypothesis was supported by calculations performed for $\rho_p = 0.5$, 1, and 10 g/cm^3 ($C = 1$ and $\rho = 1.2 \cdot 10^{-3}$ g/cm^3) at velocity ratios of $\bar{U}/U_o = 0.1$ and 5 (with Re = 300 and the ultra-Stokesian drag law). When interception corrections were made (as suggested in the following subsection), the high- and low-density results for A_i differed by < 2% from the unit-density result. Under similar conditions, these results suggest that the density ratio plays only a minor role in determining A_i, and so we have taken the unit-density value in all the calculations which follow ($\rho/(\rho_p C) = 1.2 \cdot 10^{-3}$).

TABLE 4. Effect of Velocity Ratio

	Re = 300	$\rho/(\rho_p C) = 1.2 \cdot 10^{-3}$		Ultra-Stokesian drag			
		Aspiration coefficient, A_i					
St	$\frac{\overline{U}}{U_o} = 5.00$	3.33	2.50	1.82	1.50	1.25	1.11
0.005	0.976	0.977	0.974	0.968	0.976	0.990	0.981
0.020	0.942	0.935	0.938	0.940	0.945	0.973	0.981
0.050	0.843	0.830	0.856	0.885	0.914	0.939	0.963
0.100	0.720	0.754	0.778	0.831	0.869	0.922	0.945
0.200	0.593	0.647	0.694	0.767	0.825	0.888	0.945
0.500	0.443	0.517	0.590	0.680	0.755	0.840	0.912
1.000	0.355	0.429	0.517	0.634	0.714	0.824	0.901
2.000	0.281	0.375	0.465	0.588	0.687	0.801	0.890
5.000	0.228	0.324	0.416	0.540	0.655	0.766	0.867
10.000	0.199	0.298	0.378	0.526	0.638	0.766	0.856
St	$\frac{\overline{U}}{U_o} = 1.00$	0.91	0.75	0.50	0.20	0.10	
0.005	1.001	1.006	1.018	1.043	1.092	1.189	
0.020	0.988	1.006	1.033	1.080	1.167	1.266	
0.050	0.988	1.006	1.063	1.155	1.342	1.501	
0.100	0.988	1.019	1.093	1.259	1.764	2.162	
0.200	0.976	1.033	1.124	1.392	2.367	3.689	
0.500	0.976	1.046	1.187	1.589	3.267	5.867	
1.000	0.976	1.060	1.235	1.716	3.854	7.262	
2.000	0.976	1.060	1.251	1.811	4.281	8.280	
5.000	0.963	1.060	1.268	1.884	4.610	9.091	
10.000	0.951	1.046	1.268	1.884	4.701	9.395	

Velocity Ratio

After completion of the preliminary investigations discussed earlier, a series of calculations were made in which the velocity ratio $\overline{U}/U_o$ was varied from 0.1 to 5 and the aspiration coefficient determined as a function of the intertial parameter St. For this set of calculations: double-fine grids were used for thin-walled tubes with Re = 300; an ultra-Stokesian drag law was applied; and a density ratio of $1.2 \cdot 10^{-3}$ (particle density of 1) assumed. The results are listed in Table 4, and presented in graphical form in Figure 2.

It is of interest to note that the data seem to violate two theoretical limits: $A_i \to U_o/\overline{U}$ as St tends to infinity, and $A_i \to 1$ for all St when $\overline{U}/U_o = 1$. The inconsistencies arise from a limitation of the theoretical result, which does not include the effect of particle interception. One suggestion for an interception correction can easily be obtained by repeating the theoretical argument with a finite-sized particle in either the infinite Stokes or isokinetic ($\overline{U} = U_o$) limit to obtain:

$$A_i = (U_o/\overline{U})(1 - D_p/d)^2, \tag{15}$$

where the interception parameter, D_p/d, is calculated using Eq. (14). The numerical results are in good agreement with Eq. (15) in each limit. Although strictly true only in the two limits mentioned, we also suggest accepting this functional form as a general description of the role of interception in the sampling process. Under this assumption, A_i would appear as the product of a point-mass aspiration coefficient (A_i^*) and the interception correction $(1 - D_p/d)^2$ where

$$A_i = A_i^* \cdot (1 - D_p/d)^2. \tag{16}$$

Earlier correlations [e.g., Eq. (5)] strictly

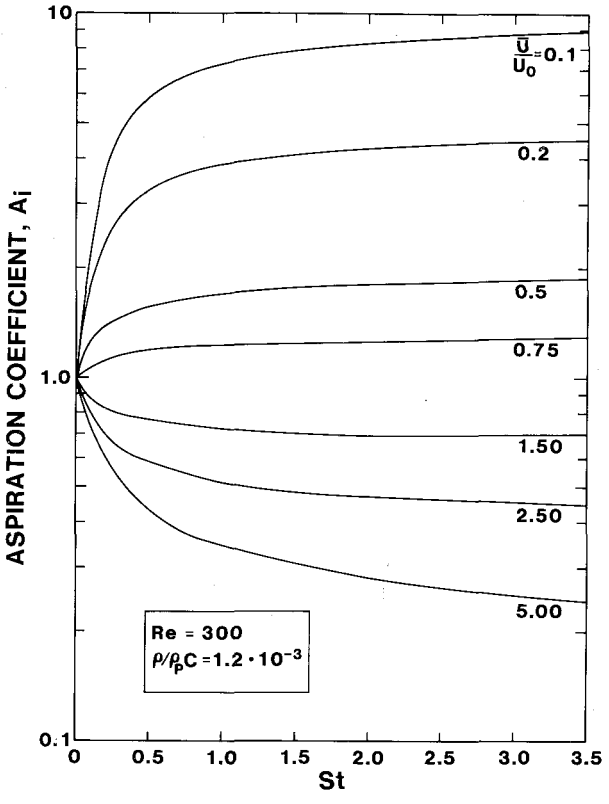

FIGURE 2. Variation of the aspiration coefficient with the Stokes number for a thin-walled probe at several values of the velocity ratio.

apply for A_i^* since they do not include any interception terms.

As shown in Fig. 3, our theoretical results are in good agreement with the experimental data of Belyaev and Levin (1972) [the numerical results have been corrected according to Eq. (16), since the interception effects in the experimental work were negligible]. Belyaev and Levin estimated their systematic errors to be 11–15% for $\bar{U}/U_o < 1$ and 7% for $\bar{U}/U_o > 1$, so that even the disagreement seen for $\bar{U}/U_o = 0.2$ is within experimental error.

We also found good agreement between our calculations for A_i^* and the correlation of Belyaev and Levin (1974) given in Eqs. (5) and (6). In the range $0.2 < \bar{U}/U_o < 5$ and $0.005 < \mathrm{St} < 10$, the correlation prediction and numerical results agreed to within a maximum error of 10%, while the average error was only 2.6% (error defined as $|A_i^* - A_{i,\mathrm{BL}}|/A_i^*$). Since the Belyaev and Levin (BL) result was obtained in turbulent flow at much higher Re than in this study, the observed agreement supports the assumptions that Re and turbulence effects are of minor importance.

Using the present numerical results, a least-squares curve-fitting method was used to investigate the dependence of k in Eq. (5) on the velocity ratio. A strong dependence on the velocity ratio was found, but the functional form was much different than in Eq. (6). For example, while Eq. (6) predicts a linear increase in k with increasing $\bar{U}/U_o$, our fitted values for k decreased with $\bar{U}/U_o$ for velocity ratios > 1. The good agreement between our results and the correlation, despite the uncertainty in k, arises from the weak dependence of A_i on k within the range of variables investigated.

Using the least-squares method, we also analyzed several other correlations. The best agreement with our results was found using

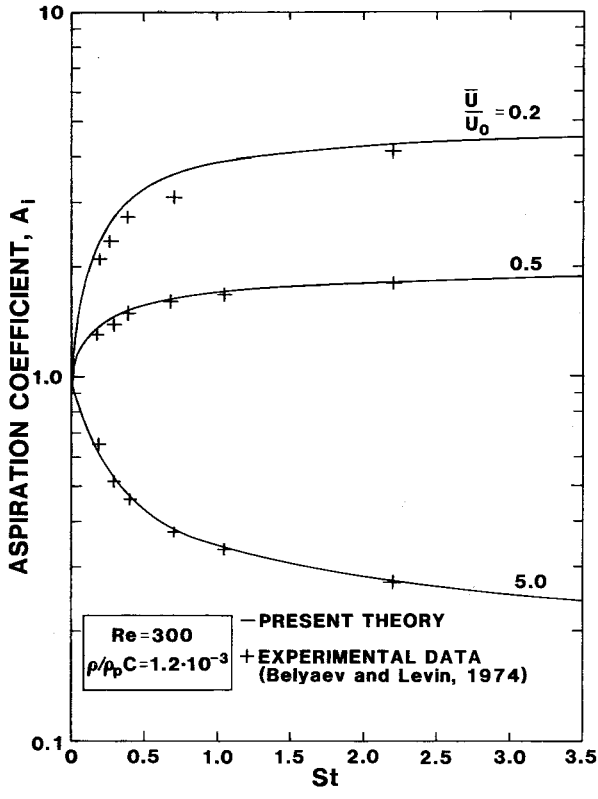

FIGURE 3. Comparison of the present theoretical result for a thin-walled probe with the experimental data of Belyaev and Levin (1974) at velocity ratios of 0.2, 0.5, and 5.0

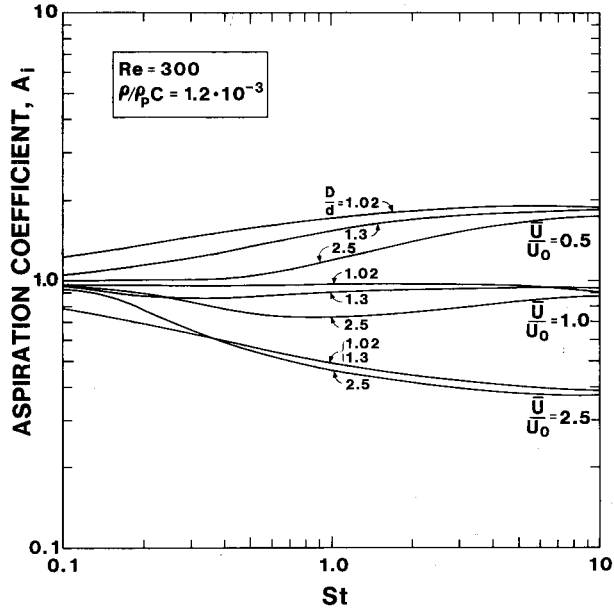

FIGURE 4. Variation of the aspiration coefficient with the Stokes number for three wall thicknesses ($D/d = 1.02$, 1.3, and 2.5) at velocity ratios of 0.5, 1.0, and 2.5

a form suggested by Selden (1977) and modified to include interception:

$$A_i^* = A_i/(1 - D_p/d)^2$$
$$= 1 + \left[\frac{U_o}{\overline{U}} - 1\right]\left[1 - \frac{1}{1 + k\mathrm{St}^n}\right]. \quad (17)$$

In the range $0.5 < \overline{U}/U_o < 5$ and $0.005 < \mathrm{St} < 10$, Eq. (17) with $k = 3.77$ and $n = 0.883$ agreed with our results to within a maximum error of 5%, while the average error was only 1.2%. For most purposes, either the Belyaev and Levin correlation or Eq. (17) will provide acceptable predictions for the aspiration coefficient.

Probe Thickness

One final series of tests were run in order to investigate the effect of probe thickness on the aspiration coefficient. Calculations were made for probe diameter ratios (D/d) of 1.02, 1.3, and 2.5 for velocity ratios of 0.5, 1.0, and 2.5. These results are given in Table 5 and shown graphically in Figure 4. The calculations show qualitative agreement with the thick-walled data of Belyaev and Levin (1972). Several observations concerning thick-walled sampling bias can be made. First, even isokinetic sampling does not insure a representative sample for thick-walled

TABLE 5. Effect of Probe Thickness

Re = 300 $\rho/(\rho_p C) = 1.2 \cdot 10^{-3}$ Ultra-Stokesian drag

		Aspiration coefficient, A_i		
D/d	St	$\overline{U}/U_o = 2.5$	1.0	0.5
1.02	0.005	0.962	0.988	1.043
	0.02	0.926	0.988	1.080
	0.05	0.856	0.976	1.136
	0.10	0.778	0.976	1.234
	0.20	0.694	0.976	1.361
	0.50	0.571	0.976	1.567
	1.0	0.517	0.976	1.716
	2.0	0.448	0.976	1.811
	5.0	0.416	0.963	1.871
	10.0	0.378	0.951	1.884
1.30	0.005	0.962	0.976	0.989
	0.02	0.950	0.976	1.007
	0.05	0.891	0.951	1.025
	0.10	0.800	0.914	1.061
	0.20	0.694	0.890	1.155
	0.50	0.571	0.890	1.351
	1.0	0.499	0.914	1.533
	2.0	0.448	0.927	1.692
	5.0	0.403	0.939	1.811
	10.0	0.378	0.939	1.847
2.50	0.005	0.974	0.976	0.971
	0.02	0.974	0.976	0.989
	0.05	0.962	0.976	1.007
	0.10	0.950	0.976	1.007
	0.20	0.789	0.914	1.007
	0.50	0.571	0.764	1.043
	1.0	0.465	0.731	1.194
	2.0	0.416	0.775	1.414
	5.0	0.378	0.843	1.657
	10.0	0.378	0.878	1.751

probes. For a probe with a diameter ratio of 2.5, a maximum in sampling bias is observed near St = 1, which is consistent with experimental observations. Second, probe thickness is seen to play a minor role for superisokinetic sampling (velocity ratios > 1). This also is in agreement with Belyaev and Levin's experimental results. Finally, for subisokinetic sampling (velocity ratios < 1), a thick-walled probe actually provides a sampling efficiency that is closer to unity than a thin-walled probe, also consistent with Belyaev and Levin's data.

CONCLUSIONS

The previous sections have presented the results of a numerical investigation of sampling bias through cylindrical probes. Both iso- and anisokinetic sampling conditions were modeled for thin- and thick-walled tubes. By assuming a low particle concentration, a dilute-solution approximation was made which permitted the separation of the problem into a flow field calculation and a subsequent particle trajectory integration. Laminar flow fields were assumed and were calculated using finite-difference solutions of the Navier-Stokes equations. Particle trajectories were then calculated by using a fourth-order Runge-Kutta method to integrate the particle equation of motion. An ultra-Stokesian drag law and particle interception were included.

Based on a dimensional analysis of the problem and on the assumptions of the physical model, five dimensionless groups (Re, $\overline{U}/U_o$, D/d, St, and $\rho/(\rho_p C)$) were identified that specify the aspiration coefficient, $A_i = \overline{C}/C_o$. Systematic investigations showed that the tube Reynolds number, Re, and the slip-modified density ratio, $\rho/(\rho_p C)$, have only a minor influence in determining A_i. Calculations were made to determine the influence of the remaining groups—velocity ratio ($\overline{U}/U_o$), diameter ratio (D/d), and Stokes number (St)—on the sampling process.

For thin-walled probes, the present results were found to be in good agreement with the data of Belyaev and Levin (1972), and with a semiempirical expression they later proposed (Belyaev and Levin, 1974). A least-squares curve-fitting method was used to determine a slightly more accurate correlation. The new correlation introduces a factor that describes the effect of particle interception.

Results for thick-walled probes were found to be in qualitative agreement with the experimental findings of Belyaev and Levin (1972). One key observation was that even isokinetic sampling does not insure a representative sample for thick-walled probes. Also, probe thickness was found to play a minor role for superisokinetic sampling (velocity ratios > 1). Finally, for subisokinetic sampling (velocity ratios < 1), a thick-walled probe actually provides a sampling efficiency that is closer to unity than a thin-walled probe.

This work was supported at the University of Minnesota by the U.S. Environmental Protection Agency under agreement EPA/CR-808319-01, and at Sandia National Laboratories by the U.S. Department of Energy under contract DE-AC04-76DP00789.

REFERENCES

Badzioch, S. (1959). *Br. J. Appl. Phys.* **10**:26–32.

Belyaev, S.P., and Levin, L.M. (1972). *J. Aerosol Sci.* **3**:127–140.

Belyaev, S.P., and Levin, L.M. (1974). *J. Aerosol Sci.* **5**:325–338.

Brady, W., and Touzalin, L.A. (1911). *J. Ind. Eng. Chem.* **3**:662–670.

Buckingham, E. (1914). *Phys. Rev.* (*2nd Ser.*) **4**:345–377.

Davies, C.N. (1968). *Br. J. Appl. Phys.* (*J. Phys. D*) **2**(1):921–932.

Davies, C.N., and Subari, M. (1982). *J. Aerosol Sci.* **13**:59–71.

Durham, M.D., and Lundgren, D.A. (1980). *J. Aerosol Sci.* **11**:179–188.

Friedlander, S.K. (1977). *Smoke, Dust, and Haze.* Wiley-Interscience, New York.

Fuchs, N.A. (1964). *The Mechanics of Aerosols.* Pergamon Press, Oxford.

Fuchs, N.A. (1975). *Atmos. Environ.* **9**:697–707.

Gosman, A.D., Pun, W.M., Runchal, A.K., Spalding, D.B., and Wolfshtein, M. (1969). *Heat and Mass Transfer in Recirculating Flows*. Academic Press, New York.

Ingham, D.B. (1981). *J. Aerosol Sci.* **12**:541–549.

Jayasekera, P.N., and Davies, C.N. (1980). *J. Aerosol Sci.* **11**:535–547.

Lipatov, G.N., Grinspun, S.A., Shingaryov, G.L., and Sutugin, A.G. (1986). *J. Aerosol Sci.* **17**:763–769.

Lundgren, D., and Calvert, S. (1967). *Am. Ind. Hyg. Assoc. J.* **28**:208–215.

Lutz, S.A., and Bajura, R.A. (1982). *Literature Review of Sampling Probes—Topical Report on Phase V: Probe Inlet Design*. Department of Mechanical and Aerospace Engineering, West Virginia University, Morgantown, WV.

Marple, V.A. (1970). *A Fundamental Study of Inertial Impactors*. Ph.D. Thesis. Mechanical Engineering Department, University of Minnesota, Minneapolis, MN.

Marple, V.A, and Liu, B.Y.H. (1974). *Environ. Sci. Technol.* **8**:648–654.

Marple, V.A., Liu, B.Y.H., and Whitby, K.T. (1974). *ASME J. Fluids Eng.* **96**:394–403.

Martone, J.A., Daley, P.S., and Boubel, R.W. (1980). *J. Air. Pollut. Control Assoc.* **30**:898–903.

Rader, D.J., and Marple, V.A. (1985). *Aerosol Sci. Technol.* **4**:141–156.

Ruping, G. (1968). *Staub-Reinhalt. Luft* **28**:1–11.

Sartor, J.D., and Abbott, C.E. (1975). *J. Appl. Meteorol.* **14**:232–239.

Sehmel, G.A. (1967). *Am. Ind. Hyg. Assoc. J.* **28**:243–253.

Selden, M.G., Jr. (1975). *Am. Ind. Hyg. Assoc. J.* **36**:549–552.

Selden, M.G., Jr. (1977). *J. Air Pollut. Control Assoc.* **27**:235–236.

Serafini, J.S. (1954). *NACA Report* 1159.

Stevens, D.C. (1986). *J. Aerosol Sci.* **17**:729–743.

Tufto, P.A., and Willeke, K. (1982). *Am. Ind. Hyg. Assoc. J.* **43**:436–443.

Van Driest, E.R. (1946). *J. Appl. Mech.* **13**:A34–A40.

Vincent, J.H. (1984). *Atmos. Environ.* **18**:1033–1035.

Vincent, J.H., Hutson, D., and Mark, D. (1982). *Atmos. Environ.* **16**:1243–1249.

Vincent, J.H., Emmett, P.C., and Mark, D. (1985). *Aerosol Sci. Technol.* **4**:17–29.

Vincent, J.H., and Mark, D. (1982). *Ann. Occup. Hyg.* **26**:3–19.

Vincent, J.H., Stevens, D.C., Mark, D., Marshall, M., and Smith, T.A. (1986). *J. Aerosol Sci.* **17**:211–224.

Vitols, V. (1966). *J. Air Pollut. Control Assoc.* **16**:79–84.

Watson, H.H., and Morris, T.G. (1952). *Engineering (London)* **174**:228–229.

Zenker, P. (1971). *Staub-Reinhalt. Luft* **31**:30–36.

Received July 6, 1987; accepted September 25, 1987